# Synthesis of Green Ferric Nanoparticles from Celery Leaves for the Dye Decolorization by Fenton Oxidation

***N. Fayyadh, Saba****[+]***; Abu Tahrim, Nurfaizah***

*Department of Chemical Sciences, Faculty of Science and Technology, Universiti Kebangsaan Malaysia, 43600 Bangi, Selangor, MALAYSIA*

**ABSTRACT:** *The creation of defiant chemical contaminants in the water is a major worry in water treatment processes. Such contaminants can never be readily eliminated with traditional treatment methods. As a result, combining adsorption with advanced oxidation processes is a critical method for removing harmful pollutants. This study aimed to investigate the efficacy of an environmentally friendly, low-cost catalyst that could be used as a heterogeneous Fenton oxidation catalyst. Ferric nanoparticles were synthesized from celery leaf extract (C-FeNPs). The Field Emission Scanning Electron Microscope (FESEM), Fourier-Transform InfraRed (FT-IR) spectroscopy, and X-Ray Diffraction (XRD) spectroscopy were used to describe the prepared catalyst. Adsorption isotherms of the chosen dye removal method were calculated and the tests were fitted with the Langmuir and Freundlich. The UV-vis spectrometer was used to determine the residual concentration of Orange Gelb (OG) dye in water. Under ideal parameters such as pH, temperature, and the concentration of OG and C-FeNPs dosage, the highest OG dye decolorization effectiveness of 99% was achieved. According to morphological analysis, nanoparticles with a diameter of 44–55 nm were shown to be responsible for the high catalytic activity. Adsorption data (R2 = 0.9436) is more consistent with the Langmuir model. Furthermore, the adsorption process was accompanied by an oxidation process more efficient.*

**KEYWORDS:** *Adsorption; Green synthesis; Nanoparticles; Heterogeneous Fenton; Water pollution; Dyes.*

## INTRODUCTION

Chemical pollution in aqueous media is a public concern, and numerous reports and assessments have shown that chemical compounds from industrial activities are extensively present in surface and underground water systems that act as sources of drinking water. As well as coexistence with dyes produced by the textile industry

***** *To whom correspondence should be addressed.*
**+** *E-mail: sabanaser02@gmail.com*
*1021-9986/2022/11/3567-3579 13/$/6.03*

in the aquatic environment and its potential effects on living organisms in general and humans in particular. Water treatment has gained a lot of attention in recent years since there are a lot of reactive dyes in different bodies of water. OG is an azo dye that is distinguished by one or more azo bonds (-N=N-) as chromophore groups connected to aromatic structures with functional groups such as –OH and $–SO_3H$ [1].

More than 50% of all widely used dyes are reactive due to their chemical stability and versatility. These commercial dyes are resistant to light degradation due to the presence of sulfonate ($SO^{3-}$) groups, are polarized, and are water-soluble [2]. Most dyes are non-biodegradable, obstruct sunlight penetration, impede photosynthesis, and raise the chemical and biological need for oxygen, water ecosystems are harmed as a result [3]. To treat wastewater, several methods such as coagulation, flocculation, sedimentation, sand filters, and aerobic and anaerobic treatments are employed. These treatments can reduce the treated effluent to acceptable levels for reuse [4]

Traditional treatment procedures are costly, time-consuming, and complex, necessitating the use of trained personnel, and these pollutants have become difficult to remove. There has been a lot of emphasis in recent years on Advanced Oxidation Methods (AOPs) for eliminating hazardous compounds and recalcitrant chemicals, dyes, and other contaminants from wastewater [5, 6]. Given the great oxidative strength of the hydroxyl radicals generated by the Fenton reaction and the prevalence of iron-rich catalysts in nature [7, 8], the heterogeneous Fenton technique is an acceptable option among the different AOPs. The use of catalysts in the Fenton method helps prevent deficiencies associated with this approach, such as a limited pH range and the production of iron sludge. Iron catalysts, on the other hand, provide advantages such as flexibility in heat and chemical processes, a short operating duration, and the ability to be reused.

Many synergies between adsorption and Advanced Oxidation Processes (AOPs) have been described, including Fenton oxidation-adsorption, ultrasound-adsorption, and ozone-adsorption [9, 10]. Adsorption was discovered by *Lowitz* (1785) and was quickly employed to remove the color from sugar during refining [11]. In the second half of the nineteenth century, activated charcoal filters were used to purify water in American water treatment plants [12].

Other resistant pollutants, including pharmaceuticals, dyes, and other organic and inorganic compounds, can be handled using mutual adsorption techniques with the Fenton process [13]. There are two common methods for combining adsorption with the Fenton process: the first uses heterogeneous multifunctional materials capable of producing ferric ions to react with the hydroxyl radical, and the second uses heterogeneous materials as adsorbents for organic materials and as a catalyst for ferric ion formation [14]. Despite the fact that adsorption is a critical component of the Fenton heterogeneous process, it is seldom mentioned that it contributes to pollutant removal [15]. The adsorption-Fenton reaction method, which uses adsorbents such as activated carbon and carbon nanotubes [16], Metal-Organic Frameworks (MOFs) [17], chitosan, and graphene [18, 19]. As a result, the debate between adsorption and Fenton oxidation is centered on these two pathways.

One of the most significant benefits of combining Fenton with adsorption is that the high dye content is swiftly destroyed by the Fenton reaction, while the residual contaminants are eliminated during the adsorption phase [20]. Many benefits exist for many types of iron nanoparticles employed as Fenton reaction catalysts, including a large surface area, being widely accessible, being stable in an acidic/basic environment, and having a stable structure at high temperatures [21, 22].

The Ferric Nano Particles (FeNPs) are an important iron source that is widely used as catalysts in the heterogeneous Fenton reaction [23]. FeNPs are a major source of iron that is frequently employed as catalysts in the heterogeneous Fenton reaction because they are less expensive and more compatible than gold, silver, and other nanoparticles [24, 25]. Because of their prospective uses and the numerous analytical methods available to describe them, these particles have attracted a great deal of interest. They oxidize extremely fast owing to the presence of $O_2$ and $H_2O$ to generate free iron ions, as shown in Eqs. (1, 2) [26]:

$$2\ Fe^0{}_{(s)} + 4H^+_{(aq)} + O_{2\,(aq)} \rightarrow 2\ Fe^{2+}_{(aq)} + 2\ H_2O \qquad (1)$$

$$Fe^0{}_{(s)} + 2\ H_2O_{aq} \rightarrow Fe^{2+}_{(aq)} + H_{2\,(g)} + 2\ OH^-{}_{(aq)} \qquad (2)$$

Numerous studies have shown that iron nanoparticles may be used successfully to cure various types of pollutants in water, for ease of transport, and can be utilized

immediately on-site, in addition to long-term activity. Because of these characteristics, nanoparticles may outperform other treatment options such as clay, hydrotalcite (anion clay), zeolites, and silica [27, 28].

Ferric nanoparticles employed as adsorbents and catalysts in the heterogeneous Fenton reaction are frequently manufactured in high quantities in a very short period by chemical processes and have a specified shape and size. One of the most significant drawbacks of chemical techniques for creating nanoparticles is that they generate sophisticated, obsolete, and expensive procedures, as well as complex waste that harms not only the environment but also human and animal health [29].

The biosynthesis of nanoparticles from plant-based supporting materials has gained significant interest in comparison with traditional adsorbents due to their abundant presence, low-cost, non-toxic nature, high performance, and environmentally friendly nature [30, 31]. The major aim of this study was to discover an efficient method for decolorizing OG dye water pollution by green synthesis nanoparticles as a catalyst for the Fenton reagent. Throughout this work, the use of green celery leaf extracts was used to synthesize FeNPs. Green celery leaves contain polyphenols that function as both a reducing and a capping agent. Celery leaves were chosen particularly for their ease of growing in huge quantities in a short period of time, as well as the Malaysian land's moist climate and great soil, which has helped to boost their output at a very low cost compared to other plants. The efficiency of removing OG was assessed by the rate of solution decolorization using a UV-Vis spectrometer.

## EXPERIMENTAL SECTION

### *Chemicals and materials*

All the chemicals used are of the highest purity, including analytical reagents, e.g., $H_2O_2$ (30%). Sulphoric acid ($H_2SO_4$) and sodium hydroxide (NaOH) have been used to modify pH, Ferrous sulfate heptahydrate ($FeSO_4.7H_2O$), Orange G dye ($C1_6H_{10}N_2Na_2O_7S_2$), anhydrous alcohol, and purified water are also used in this research. All of these chemicals were purchased with purities of more than 99.5 % from Merck & Co. Uh, Ltd. Water (DIW) used was supplied by Easy Pure Rodi (U.S.A). Celery leaves from Malaysian farms to produce nanoparticles are utilized as a catalyst in the Fenton reaction.

### *Preparation of dye solution & Fe NPs using celery leaves extract*

Experiments are performed to prepare OG solution, C-FeNPs as well as heterogeneous Fenton reagent. The dye solution was prepared in ideal conditions by dissolving 1 g of OG in a 1000 mL beaker with deionized water. Preparation experiments were conducted at a natural temperature of 25 ± 2 ℃. Measurement of the dye concentration was performed using the UV/Vis spectrophotometer (Shimadzu-1601 PC). Fe NPs can be readily synthesized using plant extracts, and this has been described in previous studies [32]. Fresh celery leaves have been collected from a Malaysian farm, were first washed with raw water for 15 min, and then washed with distilled water. After that, the leaves were dried in the oven at 50 °C for 10 min. 250 g of celery leaves were used, cut into small pieces, and dried, boiled with 500 mL of water for a maximum period of 20 min. The extract was filtered, collected, and stored at 4 °C for subsequent use. In a 100 mL volumetric flask, 0.5 g of $FeSO_4.7\ H_2O$ was dissolved with distilled water. C-FeNPs were synthesized using a 1:2 ratio of celery leaf extract. The immediate change in color of the solution from yellow to brown indicates the formation of C-FeNPs as shown in Fig. 1. FeNPs were used as catalysts in the Fenton reaction and 33% $H_2O_2$ in 100 mL of DI,5 mL of $H_2SO_4$ concentrate was added to adjust the pH of the solution. The Freundlich and Langmuir models were used to characterize the adsorption surfaces and the effectiveness of the adsorbents in order to study the adsorption property.

A mass of 1 g of potassium nitrate ($KNO_3$) was dissolved in 100 mL of water. A volume of 25 mL of 0.1 M KNO3 was taken in a series of flasks, and the initial pH (pHi) was adjusted to (2.5, 4, 6.8, and 10) by adding 0.1 N NaOH or 0.1 N hydrochloric acid (HCl). To each flask, 10 mg of nanoparticles were added, and the sample solutions were left for 24 h at 25 ± 3°C.Then, the final pH (pHf) of each flask was measured. The zero-charge point was calculated by plotting DpH (difference final and initial pHs) against the initial pH value (pHi) [33].

### *Characterization of C-FeNPs*

C-FeNPs were characterized using FESEM/EDX, XRD, and FT-IR techniques. The mineral phases were detected in the samples using X-Ray Diffraction (XRD) spectroscopy analysis using (Philips X'Pert Pro XRD),

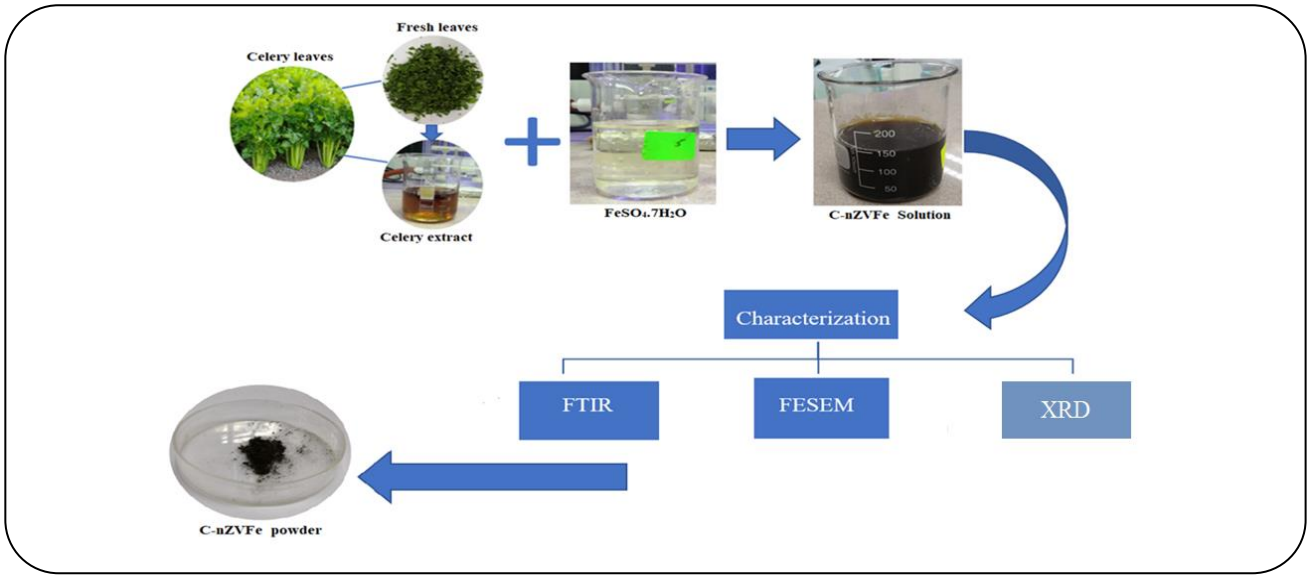


***Fig. 1: Stages of preparing Ferric nanoparticles from celery leaves.***

each sample was scanned from 10 to 70 degrees in the (2θ) range. The surface morphology of the C-FeNPs samples was examined prior to chemical oxidation using a FESEM/ EDX field emission scanning electron microscope (ZEISS, Merlin Compact Model Germany), and their primary images and contents were recorded at several enlargements. Fourier transform infrared spectroscopy (FT-IR), PerkinElmer Spectrum 400 in the ATR-FT-IR model, infrared spectra recorded in the range 4000-400 $cm^{-1}$ were used to explain the functional group responsible for reducing, covering, and stabilizing C-FeNPs. The pH point zero charge (pHpzc) of the C-FeNPs was determined using the pH drift method.

### *Analytical techniques of OG dye treatment*

The properties of the OG dye solution were determined before and after the heterogeneous Fenton process according to the basic methods for analyzing wastewater and drinking water established by the American Public Health Association (APHA 2005). The Fenton cycle is performed five times, with the pH value adjusted. The effect of parameters affecting the OG color decomposition process was studied by the inhomogeneous Fenton process, including the initial concentration of the dye, the catalyst, hydrogen peroxide, pH, and temperature. The OG dye concentration was determined using a Shimadzu model UV/Vis spectrophotometer with a wavelength range of 200 to 500 nm. The maximum wavelength in the OG solution (λ max) was 478 nm. The equilibrium concentrations and removal efficiency (%) of the dye were calculated according to Eqs. (3) and (4), respectively. Meanwhile, all experiments were performed five times and final results were presented as mean values.

$$\text{Decolorization efficiency (\%)} = \frac{(\text{Co} - \text{Ct})}{\text{Co}} \times 100\% \quad (3)$$

$$\text{qe} = (\text{Co} - \text{Ce})\text{V}/\text{m} \quad (4)$$

Equilibrium data were then fitted using the Langmuir and Freundlich models type isothermal models.

## RESULTS AND DISCUSSION

### *Characterization of the C-FeNPs*

FESEM/ EDX images a spectrum of C-FeNPs is shown in Fig. 2. C-FeNPs tend to be an inconsistent cluster, and also display some distraction, with a particle diameter of about 44 to 55 nm. The EDX spectrum includes the high peaks of C, P and S as well as of Fe and O. The C peak is mainly attributed to the polyphenol groups in the C-FeNPs that have been synthesized from celery extracts. The content of the elements in manufactured iron nanoparticles was estimated by EDX and was 45.6% C, 28.1% O, 6.5% P, 1.9% S and 17.0% Fe as shown in Fig. 3. These values can help estimate the atomic content in C-FeNPs for surface and sub-surface regions. The highest peaks indicate the presence of carbon and oxygen, and this indicates the presence of polyphenols, one of the important organic components in the green and necessary plants, in the stability of C-FeNPs. In addition to the iron summit,

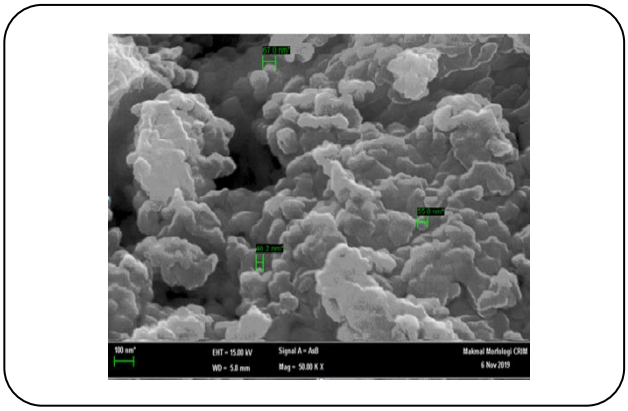

*Fig. 2: FESEM micrograph of C-FeNPs.*

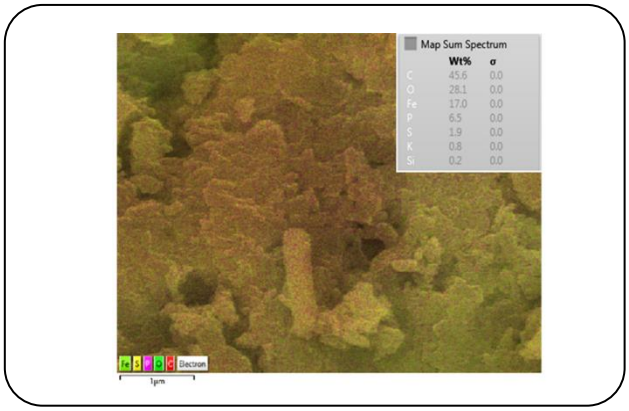


*Fig. 3: EDX spectrum of C-FeNPs.*

which indicates the iron content, which is the main element in the prepared nanoparticles.

FT-IR spectra of C-FeNPs revealed numerous peaks in the 400–4000 $cm^{-1}$ spectral region (Fig. 4). The stretching frequency of C – O – C corresponds to the high value of 1065 $cm^{-1}$. The bandwidth at 3779–3415$cm^{-1}$ was ascribed to O–H stretching vibration, indicating the presence of polyphenols, which might increase material stability [34]. Furthermore, the height of around 1650 $cm^{-1}$ may be attributed to the stretching of the C–C ring in polyphenols. After filtration and washing of the sample with ethanol, XRD also characterized the structure of the C-FeNPs.Fig. 5 indicates the XRD pattern of the material in which the peaks at 2θ of 17.88 correspond to the C-FeNP polyphenols; the peaks at (2θ) of 32.5 and 26 reflect ($Fe_3O_4$) respectively, the findings corresponded to [35]. Some peaks at (2θ) of 23 -25 present the existence of iron oxyhydroxides (FeOOH) due to fractional oxidation of the synthesis.

### *Optimum parameter effect of adsorption and heterogeneous Fenton*

*Effect of Dosage of C-FeNPs*

The effect of C-FeNPs dosages on the percentage removal of OG dye has been shown in Fig. 6. It followed the predicted pattern of increasing percentage decolorization as the dosage was increased and reached a saturation level at high doses. This is probably because the resistance to mass transfer of dye from the bulk liquid to the surface of the decolorization of OG dye increased when the dosage was changed from 5 to 35 mg/L. As the doses of adsorbent increase, the surface area available to adsorb dye increases. As expected, at a constant initial concentration of dye, increasing the sample dose provides a greater surface area and a larger number of sorption sites, hence enhancement of dye uptake [36]. The primary factor explaining this characteristic is that adsorption sites remain unsaturated during the adsorption process, whereas the number of sites available for adsorption sites increases by increasing the adsorbent dose [37]. The solid/solution ratio is an important factor determining the capacity of an adsorbent in a batch adsorption study. It is apparent that the decolorization of dye increased with increasing the amount of C-FeNPs. However, the decolorization of OG decreased with increasing the solid/solution ratio. The continuous increase of C-FeNPs causes sludge formation, which slows and then stops the oxidation reaction. Because the excessive amount of $Fe^{2+}$ in the heterogeneous Fenton solution promotes needless hydroxyl ion usage, which has a negative effect on the OG dye's oxidative decomposition. An optimal absorption dose of 35 mg/L. Based on both the adsorption potential and the rate of the OG decolorization, was selected in all additional trials.

*Effect of pH*

Five initial pH values (2.5, 4, 6.8, and 10) were examined while keeping other parameters and dosages constant (C-FeNPs = 35mg, .$H_2O_2$ = 9 mg/L, OG concentration of 100 mg/L, and T = 25 ℃). pH has a significant influence on the adsorption procedure and Fenton oxidation. The optimum pH for OG decolorization is shown in Fig. 7. From the results, it can be seen that the maximum decolorization efficiency (99%) was obtained at pH 2.5-4, which is attributed to the rise in the number of hydroxyl radicals (ȮH) produced from the decomposition of $H_2O_2$ by C-FeNPs. Increasing the number of (ȮH) leads

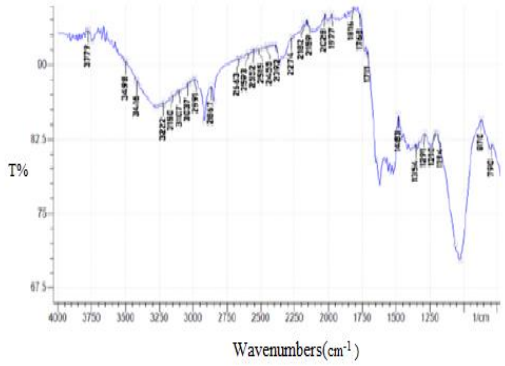


*Fig. 4: FT-IR spectrum of C-FeNPs.*

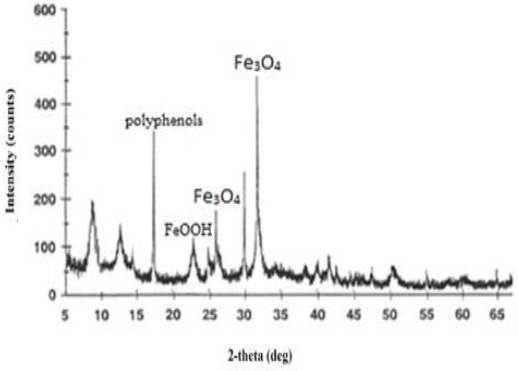


*Fig. 5: A typical XRD pattern of C-FeNPs.*

to an increase in the release of $Fe^{2+}$ ions from the C-FeNPs catalyst at higher pH levels as well as increasing the attractive forces between OG dye anions and positively charged C-FeNP surface areas.

The decolorization efficiency decreases from 99-55% gradually at pH 4-10. The pH affects the decomposition activity of both ferric ions and hydrogen peroxide. When pH >4, $Fe^{3+}$ is formed instead of $Fe^{2+}$, which reacts more slowly with hydrogen peroxide and thus produces fewer reactive hydroxyl radicals, lowering the decolorization efficiency, as reported by [38]. In addition to the fact that the surface of C-FeNPs is negatively charged at higher pH levels, the effect of electrostatic repulsion between the surfaces of negatively charged and negatively charged C-FeNPs to the dye molecules reduces the effectiveness of color adsorption. The pHpzc of C-FeNPs was determined to be 4.5. According to previous research, anion dye adsorption is equally enhanced at pH values less than pHpzc[39].

### *Effect of $H_2O_2$*

Studies on the influence of hydrogen peroxide dosing were conducted using five doses of different quantities (1.5, 5, 9, 14, and 18 mg/L) where the operating conditions were: 100 mg/L of OG dye, pH = 4 and 35 mg/L of C-FeNPs. The results were presented in Fig. 7, it was found that raising the amount of $H_2O_2$ from 1.5 to 9 mg/L contributed to improving the color removal from OG by 74% to 98% during 20 min of reaction. This rise in the removal rate can be explained by increasing the initial concentration of $H_2O_2$ due to an increase in the number of hydroxyl radicals from the rapid degradation of $H_2O_2$ [40]. Furthermore, raising the quantity of $H_2O_2$ enhances the adsorption of OG on the surface of C-FeNPs by increasing the formation of hydroxyl radicals that react with $Fe^{2+}$ produced by C-FeNPs, which has a better decolorization efficiency than OG dye. Whereas, by rising the concentration of $H_2O_2$ from 9 to18 mg/L, the rate of decolorization reported a noticeable decrease from 98% to 55%, and the reason for this from the point of view of decomposition mechanics is the increased generation of $\dot{O}OH$ radicals, which are considered to be less efficient than hydroxyl radicals, formed as a result of excessive $H_2O_2$ scavenging as seen in Eq. (5).

$$\dot{O}H + H_2O_2 \rightarrow \dot{O}OH + H_2O \quad (5)$$

Furthermore, the excess adsorption of $H_2O_2$ molecules on the composite surface of C-FeNP can create an unfavorable condition for specific adsorption of dye molecules as expected. For further oxidation experiments, the optimum condition is set at 9 mg/L of $H_2O_2$.

### *Effect of temperature*

The effects of temperature ranging from 25℃ to 50℃ on OG decolorization were examined in this study. Fig. 9 shows that raising the temperature has an advantage in the decolorization of OG, and the time required to decolorize OG was considerably shorter at higher temperatures. When the temperature was raised from 25 to 50 ℃, for example, the effectiveness of decolorization of OG increased from 38 to 96 % in 20 min. Higher temperatures increase the rate of $^{\bullet}OH$ production, which speeds up the heterogeneous Fenton oxidation process and hence improves OG decolorization [41]. Furthermore, higher temperatures may increase the adsorption rate of OG and $H_2O_2$ by increasing their diffusion rate at the solid/water interface.

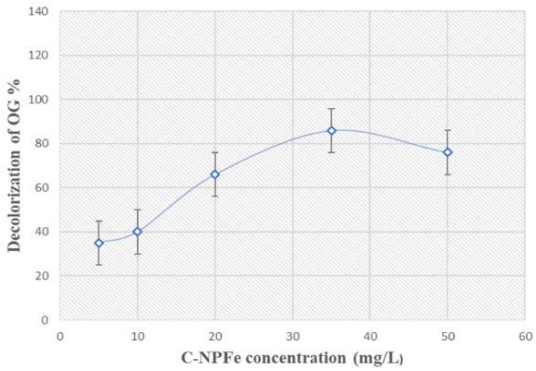


*Fig. 6: Effect of adsorbent dosage on the adsorption of OG on C-FeNPs (initial OG concentration 100 mg/L; initial $H_2O_2$ concentration 9 mg/L; T = 25°C; time: 20 min).*

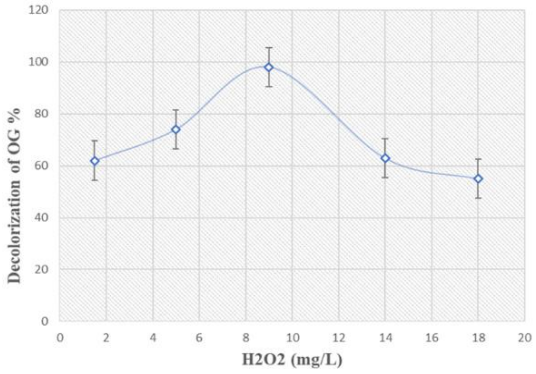


*Fig. 8: Effect of $H_2O_2$ concentration on the OG decolorization (initial OG concentration: 100 mg/L, C-FeNPs dosage: 35 mg/L; T = 25 ℃; time: 20 min).*

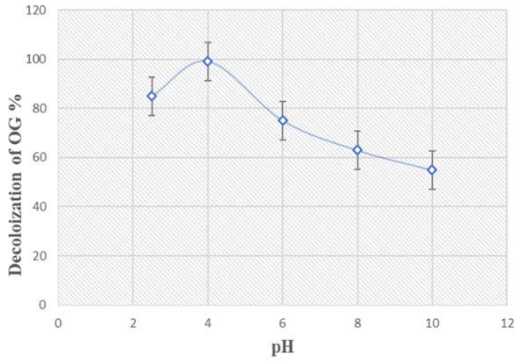


*Fig.7: Effect of pH on the OG decolorization efficiency (initial OG concentration: 100 mg/L; C-FeNPs dosage: 35 mg/L; T = 25*℃*; time: 20 min).*

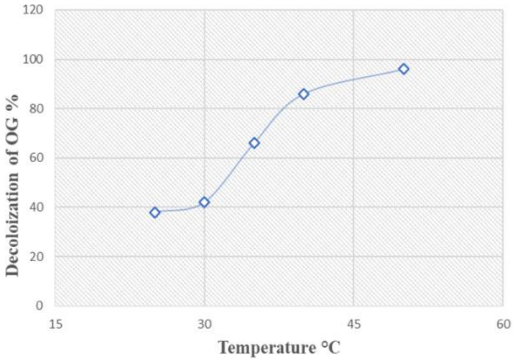


*Fig. 9: Effect of temperature on OG decolorization (initial OG concentration 100 mg/L; initial $H_2O_2$ concentration 9 mg/L; C-FeNPs dosage 35 mg/Land time: 20 min).*

### *Effect of initial OG concentration*

The influence of the primary OG concentration on the dye decolorization rate was studied in the range (10–100) mg/L at contact for 10 min without adjusting the initial pH of the medium. The impact of the prime OG dye concentration on the performance of the heterogeneous Fenton process is shown in Fig. 10. The results showed that a rise in the prime dye concentration from 10 to 100 mg/L resulted in the decolorization rate decreasing from 98% to 87%. The generation of hydroxyl radicals on the surface of the catalyst may be reduced at higher dye concentrations because the active sites of the catalyst may be occupied by the dye molecules. The efficiency of the decolorization process was reduced due to an increase in the number of dye molecules and an insufficient concentration of active radicals. [42].

Furthermore, the ability of OG adsorption to C-FeNPs decreases at the prime concentration of 10 mg/L, where the effective sites on the surface of the adsorbents are not occupied and limited to a low concentration compared to the high concentration of 100 mg/L. As shown in Fig 10, an increase in the initial dye concentration leads to a decrease in the decolorization percent and an increase in the adsorption capacity of the dye on C-FeNPs.

### *Adsorption isotherms*

Adsorption is the accumulation of a mass transfer process that may be roughly defined as the material at the interface of solid and liquid phases. Adsorption isotherms describe equilibrium relationships between the ratio of the amount adsorbed to that remaining in the solution at a given temperature at equilibrium. Isotherm data should be appropriately fit into various isotherm models to find an acceptable model that can be used in the design phase [43]. The parameters derived from the various models offer critical information on the adsorption processes,

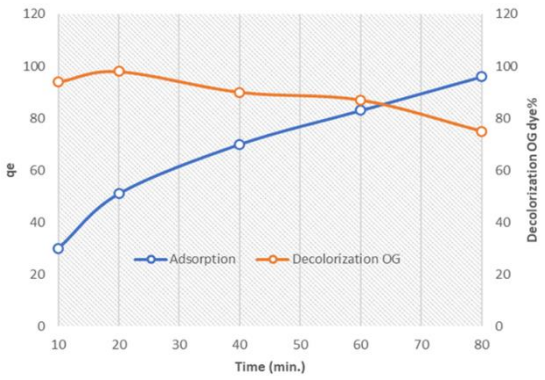


***Fig. 10: Effect of prime OG concentration on decolorization efficiency (C-FeNPs dosage 35 mg/L; T = 25℃; time: 20 min).***

surface characteristics, and affinities of the adsorbate. Linear regression is commonly employed to identify the best-fitting isotherm, and the applicability of isotherm equations is judged by comparing the correlation coefficients (R2).

The adsorption of OG on C-FeNPs was modeled using the Langmuir and Freundlich equations, which are the most common isotherm applications used for water treatment, under predefined conditions of pH, concentrations, adsorbent dose, and temperature [44]. Using different concentrations of OG dye (10-100) mg/L with 35 mg/L of C-FeNPs at for 20 min at PH = 4. The absorbance of the dye solution was determined using UV–Vis spectrometer at 200 - 500 nanometers. The equilibrium concentration was calculated and the adsorption isotherm of the OG was determined by graphically depicting the slope between the adsorption range ($\log q_e$) and the balance of the equilibrium concentration. Eq. (6) expresses the linear form of the Langmuir equation:

$$C_e/q_e = 1/(K_L q_{max}) + C_e/q_{max} \quad (6)$$

$q_e$ represents the amount of OG adsorbed over C-FeNPs at equilibrium (mg/g); $q_{max}$ is the concentration of the solution equilibrium (mg/L); is the upper bound of the dye that can adsorb to the C-FeNPs weight unit (mg/g) which is the constant value associated with the absorption capacity; KL is the adsorption equilibrium constant related to the affinity of the active sites of dye and the adsorption energy.

Table 1 reveals that the highest adsorption the correlation coefficient (R2) was 0.9436, which is in line with the Langmuir isotherm and indicates that adsorption is beneficial for OG dye decolorization. The Langmuir isotherm assumes that the adsorbent on the solid C-FeNPs surface is a monolayer, with uniform adsorption energy, and no transmigration of the adsorbents into the surface plane. The Freundlich isotherm was found to be sufficiently consistent with linear correlations (R2) in the experimental data for orange G dye. The Freundlich isotherm can be expressed by the following Eq. (7):

$$\log(x/m) = \log K + 1/n \log(C_e) \quad (7)$$

x/m represents the amount of OG adsorbed by the unit mass of the adsorbate. $C_e$ is represented by the concentration of the equilibrium and the constants are 1/1n. Where K is concerned with the degree of adsorption, and n is the temporary rate of adsorption. The Freundlich isotherm representing the C-FeNPs adsorption of OG dye has been summarized in table 1. The Freundlich constant analyzed from the linear equations, the exposure values of 1/n were within 0-1, indicating good adsorption at all temperatures measured. Despite high R2 values, the findings suggest that the Freundlich model is less consistent with experimental data than the Langmuir model, which exhibits high linearity as seen in Fig.11 (a and b). The adsorption data matches the Langmuir isotherm well, with the highest R2 in their categories (Table 1), and the maximum adsorption ability is 3.448 mg/g, showing that a Langmuir study is more appropriate. These findings are consistent with those of [45].

***Mechanism of catalytic oxidation and adsorption***

The C-FeNPs material demonstrated better activity for Fenton chemical oxidation of OG by $H_2O_2$, where the C-FeNPs material serves as a source of $Fe^{+2}$ ions. The central strategy for both heterogeneous Fenton and adsorption involves oxidative interaction between $Fe^{2+}/Fe^{3+}$ ions and $H_2O_2$; both processes are expected to participate in OG degradation simultaneously. In the adsorption process, the OG dye is easily adsorbed to the surface of the C-FeNPs, therefore, triggering some oxidation reactions in the catalytic surface that may accelerate the decolorization process.

The first stage of a series of reactions starts with hydroxyl radicals (•OH) being formed from $Fe^{2+}$ reactions from C-FeNPs and $H_2O_2$ to $Fe^{3+}$. The second stage occurs when $H_2O_2$ adsorption occurs on the surface to form

***Table 1: Isotherm parameters for the adsorption of OG dye.***

| Parameters | Freundlich | Langmuir |
|---|---|---|
| | n= 2.4 | $q_{max}$ (mg $g^{-1}$) = 3.448 |
| $R^2$ | $R^2$ (Liner)= 0.8982 | (Liner)= 0.9436 |
| | Non liner | |
| Error | | |
| CHI | 1.3733 | 0.0203 |
| ERRSQ | 2.1924 | 0.4773 |
| HYBRD | 1.1013 | 0.0212 |
| MPSD | 0.8914 | 0.0006 |
| ARE | 1.2522 | 0.0465 |
| EABS | 2.0077 | 1.2191 |
| Error sum | 6.632 | 1.7862 |

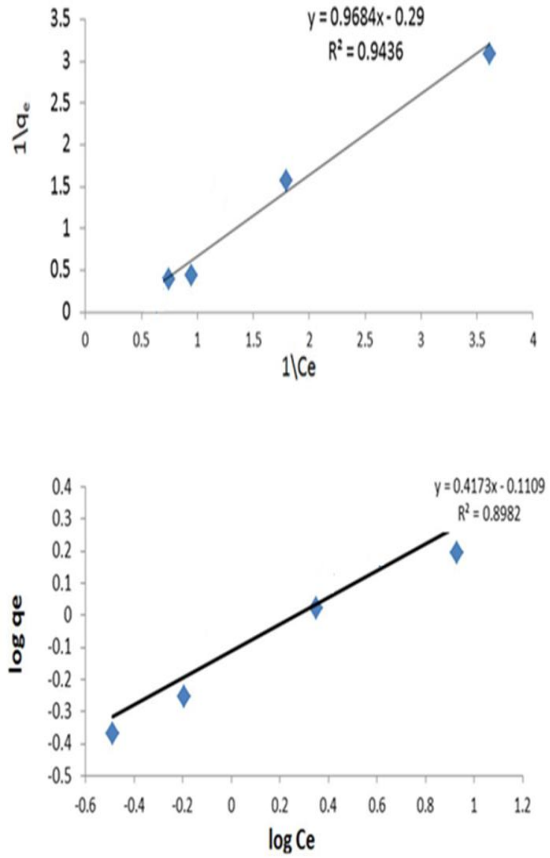


***Fig. 11: (a) Langmuir for Orange G contributing component, (b) Freundlich for Orange G contributing component.***

the matrix of the oxidized substance $Fe^{+3}$. As a result, ($HO_2^{\cdot}$) radicals are formed after $Fe^{+3}$ to $Fe^{+2}$ being reduced and the cycle is thus terminated [46]. Lastly, the $^{\cdot}OH$ and $HO_2^{\cdot}$ radicals formed as in associate and decolorize with OG dye molecules, as these radicals lead to the oxidation of adsorbed and non-adsorbed substrates by creating simple substances such as carbon dioxide and water as shown in Fig. [12].

***Reusability and stability of C-FeNPs as prepared***

Given that the economic aspect is very important in water treatment operations, therefore, both recyclability and durability are among the primary factors to be tested in the adsorbents applied in the synergistic process between the Fenton-adsorption reactions. The regeneration and re-use of C-FeNPs prepared in the heterogeneous Fenton process under improved conditions has been estimated in five consecutive trials. After a 20 min adsorption/Fenton oxidation experiment with 100 mg/L of OG dye, the compound was recovered by centrifuging C-FeNPs from the interaction admixture and washing with ethanol alcohol to remove the remaining substance, as shown in the experiment section. C-FeNPs was subjected to another reaction after it had dried up; the process had already been repeated for 5 cycles. The amount of dye and dissolved iron ($Fe^{2+}$) were then calculated to determine the reusability and stability of the compound NPs, respectively. The fact that it was found that the yield of the catalyst remained the same without measurable loss. Via experiments, the study concluded that the efficiency of OG removal in the heterogeneous Fenton system remained virtually unchanged for five successive cycles these result consistent with recent studies [47]. In addition, that the OG decolorization rate was still around 99%, to 96 %, which decreased significantly in the last two periods only compared to that of the first period, Fig. 13. This limited loss in dye removal efficiency may result from the loss of mass of $Fe_3O_4$ or from the incomplete removal of remaining by-products and reagents from active catalysts during the washing and drying process. These findings indicate that C-FeNPs, in addition to the compound's good physical and chemical stability under the experimental conditions of this study, maybe a cost-effective catalyst for removing OG in the simultaneous presence of the Fenton reaction, due to its remarkable regeneration performance.

***Table 2:***

| Method | Reaction time (min) | pH | Initial Co. OG (mg/L) | Decolorization Efficiency (%) | Ref |
|---|---|---|---|---|---|
| Adsorption by ODA nano clay | 120 | 3 | 50 | 97 | [48] |
| Heterogeneous photo-Fenton catalyst | 90 | 3 | 25 | 89 | [49] |
| Fenton-like | 120 | 5.5 | 100 | 99.7 | [50] |
| Sono-advanced Fenton | 180 | 3 | 10 | 90 | [51] |
| Fenton -catalyst (C-FeNPs) | 20 | 4 | 100 | 99 | Current work |

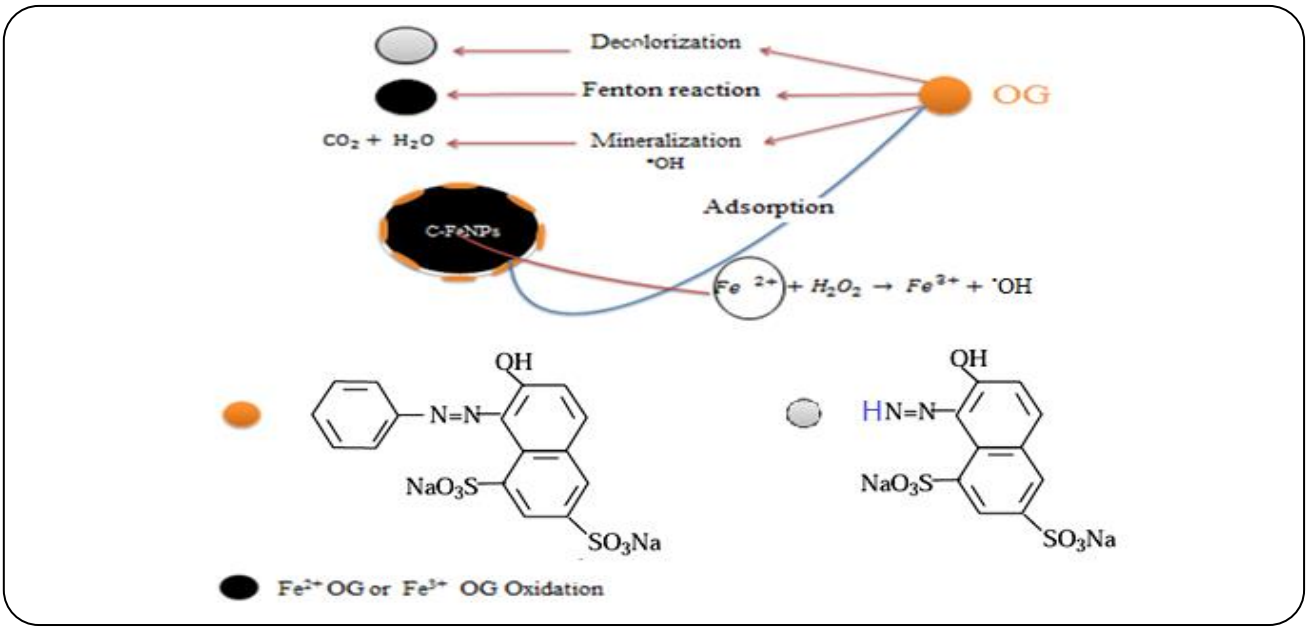


***Fig. 12: Proposed mechanism for the decolorization of OG onto C-FeNPs.***

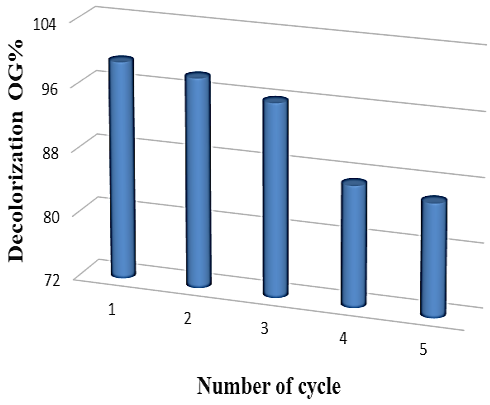


***Fig. 13: Recycle of C-FeNPs Fenton in decolorization of OG dye.***

***Comparison of reaction efficiency with previous studies***

Based on previous relevant studies, a comparative assay was performed to highlight the higher efficiency of the decolorization of OG from aqueous solutions (Table 2). Considering different treatment approaches, the results show that C-FeNPs as a catalyst in the Fenton reaction have a high propensity to decolorize OG from wastewater, using a low-cost, quick to prepare, and simple to use technique to synthesize catalysts under uncomplicated conditions.

## CONCUSIONS

Celery leaf extract was used in this study to generate C-FeNPs, a novel catalyst. A parametric investigation of Fenton oxidation employing C-FeNPs revealed that increasing the catalyst and hydrogen peroxide dosages, as well as the temperature, increased the rate of OG decolorization. On the other hand, increasing the pH of the solution decreased the yield of decolorization OG. When the pH value was 4, Fenton's reagent conditioning combined with adsorption considerably increased dye decolorization performance. The adsorption capacity

of dye increased as the starting dye concentration increased, but the maximum adsorption capacity dropped as the temperature climbed. Fitting equilibrium data to Langmuir and Freundlich isotherms revealed that the Langmuir model was better suited for describing Orange G adsorption, which has a monolayer adsorption capacity of 3.448 mg/g. According to the findings of this study, C-FeNPs are a green alternative strategy that can result in advancements in wastewater treatment and high-quality treated effluent.

**acknowledgment**

The authors would like to warmly thank the National University of Malaysia's Makmal Morfologi CRIM for their support.

*Received: Sep. 23, 2021 ; Accepted: Jan. 3, 2022*

**REFERENCE**

[1] Garcia-Segura S., Dosta S., Guilemany M. J., Brillas E., Solar Photoelectrocatalytic Degradation of Acid Orange 7 Azo Dye Using a Highly Stable TiO2 Photoanode Synthesized by Atmospheric Plasma Spray, *Applied Catalysis B: Environmental*, **132**: 142-150 (2013).

[2] Obaid M.K., Chuah Abdullah L., Jabir Idan I., Removal of Reactive Orange 16 Dye from Aqueous Solution by Using Modified Kenaf Core Fiber, *Journal of Chemistry*, **2016** (2016).

[3] Lima Santos Klienchen Dalari B., Lisboa Giroletti C., Dalri-Cecato L., Gonzaga Domingos D., Nagel Hassemer M.E., Application of Heterogeneous Photo-Fenton Process Using Chitosan Beads for Textile Wastewater Treatment, *Journal of Environmental Chemical Engineering*, **8(4)**: 103893 (2020).

[4] Khataee A.R., Zarei M., Khataee A.R. Electrochemical Treatment of Dye Solution by Oxalate Catalyzed Photoelectro-Fenton Process Using a Carbon Nanotube-Ptfe Cathode: Optimization by Central Composite Design, *Clean–Soil, Air, Water*, **39(5)**: 482-490 (2011).

[5] Gao Y., Guo Y., Zhang H. Iron Modified Bentonite: Enhanced Adsorption Performance for Organic Pollutant and its Regeneration by Heterogeneous Visible Light Photo-Fenton Process at Circumneutral pH, *Journal of Hazardous Materials*, **302**: 105-113 (2016).

[6] Bao S., Shi Y., Zhang Y., He L., Yu W., Chen Z., Wu Y., Li L., Study on the Efficient Removal of Azo Dyes by Heterogeneous Photo-Fenton Process with 3D Flower-Like Layered Double Hydroxide, *Water Science and Technology*, **81(11)**: 2368-2380 (2020).

[7] Xu M., Wu Ch., Zhou Y., "Advancements in the Fenton Process for Wastewater Treatment", *Advanced Oxidation Processes*, **61** (2020).

[8] Drumm F.C., Schumacher de Oliveira J., Luiz Foletto E., Luiz Dotto G., Marlon Moraes Flores E., Enders M.S.P., Irineu Mueller E., Luiz Janh S., Response Surface Methodology Approach for the Optimization of Tartrazine Removal by Heterogeneous Photo-Fenton Process Using Mesostructured Fe2O3-Suppoted ZSM-5 Prepared by Chitin-Templating, *Chemical Engineering Communications*, **205(4)**: 445-455 (2018).

[9] Bazrafshan A.A., Ghaedi M., Hajati Sh., Naghiha R., Asfaram A., Synthesis of ZnO-Nanorod-Based Materials for Antibacterial, Antifungal Activities, DNA Cleavage and Efficient Ultrasound-Assisted Dyes Adsorption, *Ecotoxicology and Environmental Safety*, **142**: 330-337 (2017).

[10] Khataee A., Kıranşan M., Karaca S., Sheydaei M., Photocatalytic Ozonation of Metronidazole by Synthesized Zinc Oxide Nanoparticles Immobilized on Montmorillonite, *Journal of the Taiwan Institute of Chemical Engineers*, **74**: 196-204 (2017).

[11] Liang R., Hu A., Hatat-Fraile M., Zhou N., Fundamentals on Adsorption, Membrane Filtration, and Advanced Oxidation Processes for Water Treatment, In Nanotechnology for Water Treatment and Purification, pp. 1-45. Springer, Cham, (2014).

[12] Crittenden J.C., Trussell R.R., W. Hand D., Howe K., Tchobanoglous G., "MWH's Water Treatment: Principles and Design", John Wiley & Sons, (2012).

[13] Azha S.F., Sellaoui L., Engku Yunus E.H., Yee C.J., Bonilla-Petriciolet A., Ben Lamine A., Ismail S., Iron-Modified Composite Adsorbent Coating for Azo Dye Removal and its Regeneration by Photo-Fenton Process: Synthesis, Characterization and Adsorption Mechanism Interpretation, *Chemical Engineering Journal*, **361**: 31-40 (2019).

[14] Meijide J., Rodríguez S., Angeles Sanromán M., Pazos M., Comprehensive Solution for Acetamiprid Degradation: Combined Electro-Fenton and Adsorption Process, *Journal of Electroanalytical Chemistry*, **808**: 446-454 (2018).

[15] Babaei B., Velasquez-Mao A.J., Thomopoulos S., Elson E.L., Abramowitch S.D., Genin G.M., Discrete Quasi-Linear Viscoelastic Damping Analysis of Connective Tissues, and the Biomechanics of Stretching, *Journal of the Mechanical Behavior of Biomedical Materials*, **69**: 193-202 (2017).

[16] Ioannidou O., Zabaniotou A., Agricultural Residues as Precursors for Activated Carbon Production—A Review, *Renewable and Sustainable Energy Reviews*, **11(9)**: 1966-2005 (2007).

[17] Yagub M.T., Kanti Sen T., Afroze Sh., Ming Ang H., Dye and its Removal from Aqueous Solution by Adsorption: A Review, *Advances in Colloid and Interface Science*, **209**: 172-184 (2014).

[18] Liu Ch., Bai R., Recent Advances in Chitosan and its Derivatives as Adsorbents for Removal of Pollutants from Water and Wastewater, *Current Opinion in Chemical Engineering*, **4**: 62-70 (2014).

[19] Ali I., Mbianda X.Y., Burakov A., Galunin E., Burakova I., Mkrtchyan E., Tkachev A., Grachev V., Graphene Based Adsorbents for Remediation of Noxious Pollutants from Wastewater, *Environment International*, **127**: 160-180 (2019).

[20] Almazán-Sánchez, Perla Tatiana, Marcos J. Solache-Ríos, Ivonne Linares-Hernández, and Verónica Martínez-Miranda, Adsorption-Regeneration by Heterogeneous Fenton Process Using Modified Carbon and Clay Materials for Removal of Indigo Blue, *Environmental Technology*, **37(14)**: 1843-1856 (2016).

[21] Pereira M.C., Oliveira L.C.A., Murad E., Iron Oxide Catalysts: Fenton and Fenton-like Reactions–A Review, *Clay Minerals*, **47(3)**: 285-302 (2012).

[22] Dhakshinamoorthy A., Navalon S., Alvaro M., Garcia H., Metal Nanoparticles as Heterogeneous Fenton Catalysts, *Chem. Sus. Chem.*, **5(1)**: 46-64 (2012).

[23] Eid R., TT Arab N., Greenwood M.T., Iron Mediated Toxicity and Programmed Cell Death: A Review and a Re-Examination of Existing Paradigms, *Biochimica et Biophysica Acta (BBA)-Molecular Cell Research*, **1864(2)**: 399-430 (2017).

[24] Mahdavi M., Namvar F., Bin Ahmad M., Mohamad R., Green Biosynthesis and Characterization of Magnetic Iron Oxide (Fe3O4) Nanoparticles Using Seaweed (Sargassum Muticum) Aqueous Extract, *Molecules*, **18(5)**: 5954-5964 (2013).

[25] Parham H., Zargar B., Heidari Z., Hatamie A., Magnetic Solid-Phase Extraction of Rose Bengal Using Iron Oxide Nanoparticles Modified with Cetyltrimethylammonium Bromide, *Journal of the Iranian Chemical Society*, **8(1)**: S9-S16 (2011).

[26] Huber D.L., Synthesis, Properties, and Applications of Iron Nanoparticles, *Small*, **1(5)**: 482-501 (2005).

[27] Ramirez J.H., Costa C.A., Madeira L.M., Mata G., Vicente M.A., Rojas-Cervantes M.L., López-Peinado A.J., Martín-Aranda R.M., Fenton-Like Oxidation of Orange II Solutions Using Heterogeneous Catalysts Based on Saponite Clay, *Applied Catalysis B: Environmental*, **71(1-2)**: 44-56 (2007).

[28] Fukuchi Sh., Nishimoto R., Fukushima M., Zhu Q., Effects of Reducing Agents on the Degradation of 2, 4, 6-tribromophenol in a Heterogeneous Fenton-Like System with an Iron-Loaded Natural Zeolite, *Applied Catalysis B: Environmental*, **147**: 411-419 (2014).

[29] Xu L., Wang J., A Heterogeneous Fenton-Like System with Nanoparticulate Zero-Valent Iron for Removal of 4-chloro-3-mthyl Phenol, *Journal of Hazardous Materials*, **186(1)**: 256-264 (2011).

[30] Patra J.K., Baek K.-H., Green Nanobiotechnology: Factors Affecting Synthesis and Characterization Techniques, *Journal of Nanomaterials*, 2014 (2014).

[31] Huang L., Weng X., Chen Z., Megharaj M., Naidu R., Synthesis of Iron-Based Nanoparticles Using Oolong Tea Extract for the Degradation of Malachite Green, *Spectrochimica Acta Part A: Molecular and Biomolecular Spectroscopy*, **117**: 801-804 (2014).

[32] Kuang Y., Wang Q., Chen Z., Megharaj M., Naidu R., Heterogeneous Fenton-Like Oxidation of Monochlorobenzene Using Green Synthesis of Iron Nanoparticles, *Journal of Colloid and Interface Science*, **410**: 67-73 (2013).

[33] Oladipo A.A., Gazi M., Targeted Boron Removal from Highly-Saline and Boron-Spiked Seawater Using Magnetic Nanobeads: Chemometric Optimisation and Modelling Studies, *Chemical Engineering Research and Design* **121**: 329-338 (2017).

[34] Sangami S., Manu B., Catalytic Efficiency of Laterite-Based FeNPs for the Mineralization of Mixture of Herbicides in Water, *Environmental Technology* (2018).

[35] Devatha C. P., Kumar Thalla A., Katte S.Y., Green Synthesis of Iron Nanoparticles Using Different Leaf Extracts for Treatment of Domestic Waste Water, *Journal of Cleaner Production* **139**: 1425-1435 (2016).

[36] Groiss S., Selvaraj R., Varadavenkatesan T., Vinayagam R., Structural Characterization, Antibacterial and Catalytic Effect of Iron Oxide Nanoparticles Synthesised Using the Leaf Extract of Cynometra Ramiflora, *Journal of Molecular Structure*, **1128**: 572-578 (2017).

[37] Truskewycz A., Shukla R., Ball A.S., Iron Nanoparticles Synthesized Using Green Tea Extracts for the Fenton-Like Degradation of Concentrated Dye Mixtures at Elevated Temperatures, *Journal of Environmental Chemical Engineering*, **4(4)**: 4409-4417 (2016).

[38] Sha Y., Mathew I., Cui Q., Clay M., Gao F., Zhang X.J., Gu Z., Rapid Degradation of Azo Dye Methyl Orange Using Hollow Cobalt Nanoparticles, *Chemosphere*, **144**: 1530-1535 (2016).

[39] Farahani M., et al., Adsorption-Based Cationic Dyes Using the Carbon Active Sugarcane Bagasse, *Procedia Environmental Sciences*, **10**: 203-208 (2011).

[40] Tiya-Djowe A., Nzali S., Njoyim E.T., Laminsi S., Gaigneaux E.M. Thermal Treatment of Plasma-Synthesized Goethite Improves Fenton-Like Degradation of Orange II Dye, *Environmental Chemistry Letters*, **14(4)**: 515-519 (2016).

[41] Santhanaraj D., Ricky Joseph N., Ramkumar V., Selvamani A., Bincy I. P., Rajakumar K., Influence of Lattice Strain on Fe 3 O 4@ Carbon Catalyst for the Destruction of Organic Dye in Polluted Water Using a Combined Adsorption and Fenton Process, *RSC Advances*, **10(64)**: 39146-39159 (2020).

[42] Banerjee S., Dubey Sh., Kumar Gautam R., Chattopadhyaya M.C., Sharma Y.C., Adsorption Characteristics of Alumina Nanoparticles for the Removal of Hazardous Dye, Orange G from Aqueous Solutions, *Arabian Journal of Chemistry*, **12(8)**: 5339-5354 (2019).

[43] Zheng X., Zheng H., Zhou Y., Sun Y., Zhao R., Liu Y., Zhang S., Enhanced Adsorption of Orange G from Aqueous Solutions by Quaternary Ammonium Group-Rich Magnetic Nanoparticles *Colloids and Surfaces A: Physicochemical and Engineering Aspects*, **580**: 123746 (2019).

[44] Zargar B., Parham H., Hatamie A., Modified Iron Oxide Nanoparticles as Solid Phase Extractor for Spectrophotometeric Determination and Separation of Basic Fuchsin, *Talanta*, **77(4)**: 1328-1331 (2009).

[45] Sravanthi K., Ayodhya D., Yadgiri Swamy P., Green Synthesis, Characterization of Biomaterial-Supported Zero-Valent Iron Nanoparticles for Contaminated Water Treatment, *Journal of Analytical Science and Technology*, **9(1)**: 1-11 (2018).

[46] Nidheesh P.V., Gandhimathi R., Thanga Ramesh Sh., Degradation of Dyes from Aqueous Solution by Fenton Processes: A Review, *Environmental Science and Pollution Research*, **20(4)**: 2099-2132 (2013).

[47] Arde S.M., et al. Synthesis of Quinoxaline, Benzimidazole and Pyrazole Derivatives under the Catalytic Influence of Biosurfactant-Stabilized Iron Nanoparticles in Water, *Research on Chemical Intermediates*, **46(11)**: 5069-5086 (2020).

[48] Salam M.A., Kosa S.A., Al-Beladi A.A., Application of Nanoclay for the Adsorptive Removal of Orange G Dye from Aqueous Solution, *Journal of Molecular Liquids*, **241**: 469-477 (2017).

[49] Wang Y., Priambodo R., Zhang H., Huang Y.H., Degradation of the Azo Dye Orange G in a Fluidized Bed Reactor Using Iron Oxide as a Heterogeneous Photo-Fenton Catalyst, *Rsc. Advances*, **5(56)**: 45276-45283 (2015).

[50] Park J.-H., Wang J.J., Xiao R., Tafti N., DeLaune R.D., Seo D.C., Degradation of Orange G by Fenton-like Reaction with Fe-impregnated Biochar Catalyst, *Bioresource Technology*, **249**: 368-376 (2018).

[51] Cai M., Su J., Lian G., Wei X., Dong Ch., Zhang H., Jin M., Wei Z., Sono-Advanced Fenton Decolorization of Azo Dye Orange G: Analysis of Synergistic Effect and Mechanisms, *Ultrasonics Sonochemistry*, **31**: 193-200 (2016).